

UDC 621.311:681.5

<https://doi.org/10.33271/nvngu/2021-5/073>

**D. V. Tugay**,  
orcid.org/0000-0003-2617-0297,  
**S. I. Korneliuk**,  
orcid.org/0000-0001-9885-1724,  
**O. O. Shkurpela**,  
orcid.org/0000-0002-7872-221X,  
**V. S. Akimov**,  
orcid.org/0000-0002-4928-5428

O. M. Beketov National University of Urban Economy in  
Kharkiv, Kharkiv, Ukraine, e-mail: [tugaydmytro@gmail.com](mailto:tugaydmytro@gmail.com)

## SIMULATION OF INDUSTRIAL SOLAR PHOTOVOLTAIC STATION WITH TRANSFORMERLESS CONVERTER SYSTEM

**Purpose.** Creation of a detailed model of a solar photovoltaic station with a converter system based on a cascaded multi-level inverter with the MPPT (maximum power point tracker) function to investigate its operating modes in distributed power systems.

**Methodology.** To carry out the research, the paper used the methods of system synthesis, mathematical and computer modeling to create photovoltaic station models and components; a physical experiment in obtaining thermal characteristics of the photovoltaic module SolarDay SDM72 360 W; modern power theories for synthesis of the vector control system of a multi-level inverter.

**Findings.** the Matlab-model of solar photovoltaic station with transformerless 29-level cascade voltage inverter is synthesized. The model confirmed the serviceability and efficiency of the converter system and the power plant as a whole. An algorithm is proposed and an MPP tracker with volt-ampere characteristics of the photovoltaic module, which corresponds to the maximum power extraction, is synthesized on the basis of the algorithm. The algorithm was validated by the model for any solar radiation intensity.

**Originality.** The total mathematical model of the photoelectric module, which accounts for its energy and heat characteristics, is obtained and can be used for simulating the operation of any computer model of the photoelectric converter under Matlab/Simulink/SimPowerSystems environment.

**Practical value.** The model results indicate the prospects of industrial implementation of transformerless multi-level converter systems to be used in the structure of powerful solar photovoltaic stations.

**Keywords:** *PV module, solar photovoltaic station, multi-level inverter, converter system, MPP tracker*

**Introduction.** Considerable interest in renewable energy has contributed to the creation of a new segment in the electricity sector, which is growing rapidly and is affecting the power industry and its development in many countries of the world. Solar photovoltaic stations, as the most common example of renewable energy, hold the leading growth rates due to the modular construction principle and facilitate the construction and operation of such facilities under favorable climatic conditions [1]. The modular topology of photovoltaic stations makes it possible to scale installed power from a few hundred watts up to a gigawatt and higher [2, 3].

Grid-based industrial solar power plants (SPP) with installed power exceeding a few megawatts are the most common. In this segment, leading manufacturers offer various technological solutions to provide the efficient delivery of solar-generated energy to the power grid. The modern development of production of powerful high-voltage semiconductor devices and converters based on them makes the implementation of various circuit design solutions possible for grid connected solar power plants. Despite this, the most traditional approaches to converter systems in industrial photovoltaics have been adopted, owing primarily to the lack of systematization of new technical solutions proposed in recent scientific publications. There is therefore a significant problem today in

the research on the characteristics, development and reporting in the scientific literature of new promising types of semiconductor power converter devices for high-power grid solar plants. One such converter is a cascading multi-level voltage inverter.

**Literature review.** The analysis of scientific publications shows that in the given power range, the most traditional solutions are the use of low-power string inverters (Fig. 1, *a*) [2, 3] or powerful grid tie inverter [2, 4, 5] (Fig. 1, *b*) to connect arrays of photovoltaic modules to the industrial network. The special feature of the organization of the power transmission systems in this case is the combination of the AC-side converters or the DC-side arrays of PV modules and the use of a network transformer for galvanic isolation of the 380 V and 6(10) kV networks [2]. An alternative is a power plant design combining arrays of single-phase alternating current photovoltaic modules [6, 7], allowing for high output voltage quality [8, 9]. This principle underlies many forward-looking topologies [10, 11], including those with an asymmetric structure [12], one of which is the use of a high-voltage multi-layer cascade converter without a network transformer (Fig. 1, *c*) [13, 14]. The absence of a transformer means that it is possible to connect solar power plants directly to the 6(10) kV grid or to 35 or 110 kV district substations through 10/110 kV high voltage step-up transformers. Furthermore, the cascading principle of the inverter build up makes it possible to solve a number of

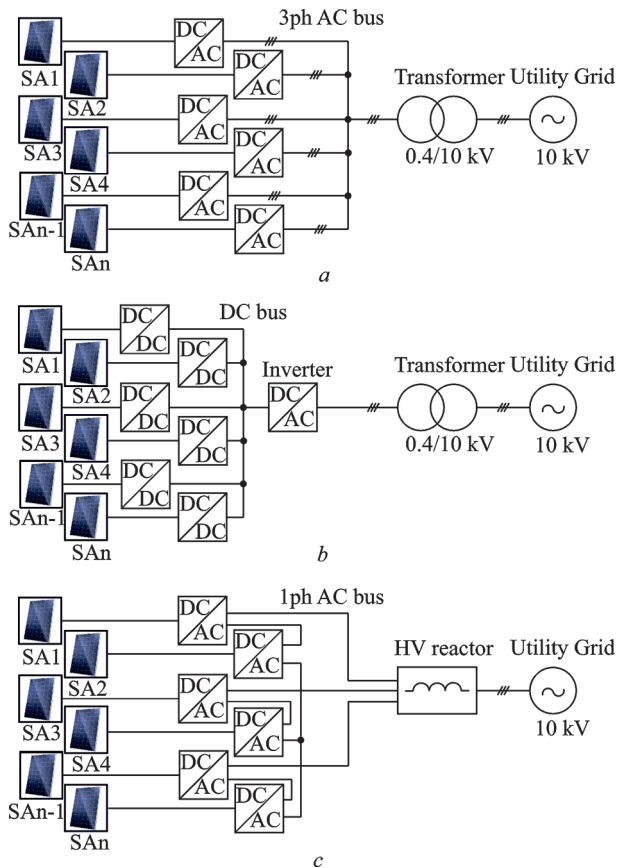


Fig. 1. Simplified circuit of photovoltaic stations:  
 a – with string inverters; b – with a single powerful inverter; c – transformerless circuit

problems, among which is the provision of an individual MPP tracker for each cell of the converter and ensuring symmetrical phase loading by the SPP generated current [13].

Disadvantages of using a common high-power converter include, for instance, different operation modes of the converter system cells [15] due to the large area of the power plant, especially in the case of variable weather conditions (clouds, precipitations, and others). Computer modeling using Matlab/Simulink/SymPowerSys [14, 16] is a reliable tool for accounting such factors. In addition, powerful software complexes allow performing simulation of complex electric power complexes' operation in different operating modes, which greatly simplifies their development at the design stage.

**Unsolved aspects of the problem.** The literature sources discussed above point to studies on individual characteristics and peculiarities of the operation of transformation systems based on multilevel cascade inverters in the structure of solar photovoltaic stations [5, 13, 14, 16]. The most commonly used models were basic blocks and solutions offered to Matlab users [14, 16]. Moreover, a review of the information sources revealed the lack of detailed models of the proposed converters that would enable to assess their performance in different operating modes of the distributed power system, considering not only the energy but also the thermal characteristics of photovoltaic cells [13, 14, 16].

The use of low-power laboratory samples [4] and their simulations [17] does not allow for a full assessment of the adequacy of the data obtained as well as for the extrapolation of the experimental results to powerful industrial systems.

Therefore, the common problem that remains to be solved consists in obtaining a detailed simulation model considered in the conversion system operation, allowing a comprehensive assessment of the prospects for its implementation.

**The purpose** of this paper is to create a detailed model of a solar photovoltaic station with a converter system based on a

cascaded multi-level inverter capable of maximum power point tracking (MPPT) to study its operation modes in distributed power systems.

To reach the goal, the following sequence of objectives should be pursued:

- to develop a detailed solar photovoltaic module model that takes into account the electrical and temperature characteristics of the photovoltaic unit;
- to implement the MPPT algorithm;
- to synthesize the intermediate PV array model with a voltage inverter, which performs the function of the MPP tracker;
- to create a complete model of the SPP based on the multilevel cascade inverter and to test its performance.

**Results.** Using the Matlab model, we will consider a photovoltaic station circuit with a rated power of 8.4 MW (Fig. 2). The conversion system of the power station consists of 42 symmetrical inverter cells (14 per phase), which schematically repeats the arrangement of the 29-level cascade multi-level voltage inverter for the high-voltage frequency-controlled electric drive [18].

A photovoltaic array of solar PV modules with the installed power of  $P_{arr} = 200$  kW is connected to the network through each cell. The array is formed by 576 Solarday SDM72 360 W modules [19, 20], which are included in  $N_p = 18$  parallel series with  $N_s = 32$  series connected modules per each (Solar Array A1 – Solar Array C14). Each of the DC photoelectric arrays is connected to a constant-voltage single-phase bridge transistor inverter (A1-C14). The inverter cells are combined in series circles (14 cells per converter phase) and are connected to the electric grid through a high-voltage inductance reactor of 5 mH. Thus, the voltage in the direct current link of the inverter cell (output voltage of the photoelectric array) is proportional to the 1/14 phase voltage of the industrial network to which the SPP is connected. The generation and distribution of control impulses on inverter cells is carried out by the vector control system of the converter (Control System), which is carried out using forward and backward coordinate transformations ( $abc-dq0$ ), which additionally implements the MPPT controller function. To efficiently filter the high-frequency component of the output currents, a small capacitor battery (C\_C\_K) with a capacity of 300  $\mu$ F is connected to the grid clamps.

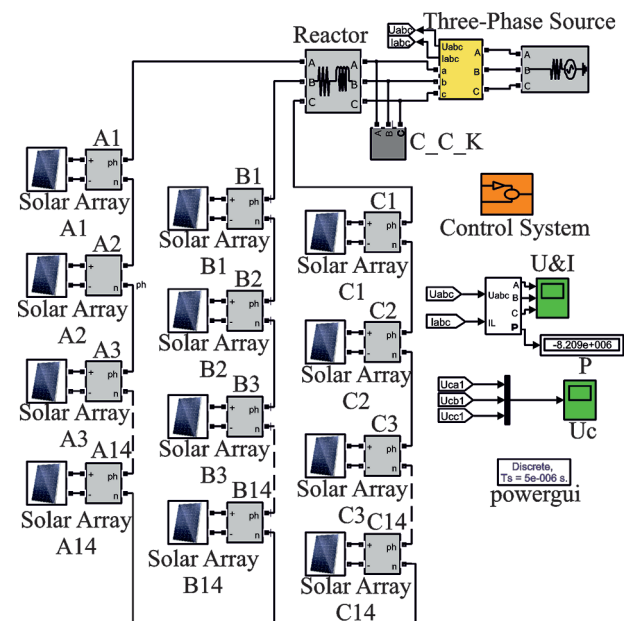


Fig. 2. Matlab-model of the photovoltaic station with rated power of 8.4 MW based on the 29-level transformerless cascade voltage converter

The array configuration can be calculated by the following ratios

$$N_s = \frac{3\sqrt{2}kU_{line}}{n \cdot V_{mpp} \cdot [1 + (T_{min} - T_n)\beta_T]};$$

$$N_p = \frac{P_n}{P_{pv} \cdot [1 - C_T(T_{PTC} - T_n)] \cdot n \cdot N_s},$$

where  $k = 1.25-1.5$ ,  $U_{line}$  is the current value of the linear voltage of the power grid to which the power plant is connected;  $n$  is the number of the converter cells;  $V_{mpp}$  is the PV module voltage at the point of maximum power extraction;  $P_n$  is the power plant rated power;  $P_{pv}$  is the PV module power;  $C_T$  is the temperature coefficient corresponding to the decrease in maximum power;  $\beta_T$  is the temperature coefficient of the module;  $T_{min}$  is the minimum operating temperature of the PV module (in winter);  $T_n = 25^\circ\text{C}$  is the nominal temperature;  $T_{PTC} = 20 + 1.389 \cdot (NOCT - 20) \cdot (0.9 - \eta_{pv})$  is the temperature of the photoelectric cell under normal conditions;  $\eta_{pv}$  is the PV module efficiency.

Given the maximum system voltage in the DC link  $U_{DCmax}$  is conventionally defined by the manufacturer of photovoltaic equipment for various types and series of PV modules (for instance, for the Solarday SDM72 360 W PV module it is 1500 V), the number of converter cells can be calculated by the ratio

$$n = \frac{3\sqrt{2}kU_{line}}{U_{DCmax}}. \quad (1)$$

Taking into account (1), the number of serially connected modules in the photoelectric array is determined by a simple ratio

$$N_s = \frac{U_{DCmax}}{V_{mpp} \cdot [1 + (T_{min} - T_n)\beta_T]}.$$

The PV module model is synthesized according to its electrical and thermal characteristics by the procedure proposed in [13].

The converter is connected to the 10 kV network without a power transformer, through the reactor  $L_s$ .

The Matlab-model of the PV module implements the solution of the current-voltage characteristic equation by the procedure described in [13] and corresponds to a detailed equivalent circuit, based on which the output current of the PV module can be determined by the ratio

$$I_p = I_{ph} - I_0 \left[ e^{\frac{q(V_p + I_p R_s)}{n \cdot K \cdot n_s \cdot T}} - 1 \right] - I_{sh}, \quad (2)$$

where  $I_{ph}$  is the photoelectric current

$$I_{ph} = \left[ I_{sc} + k_i(T - 298) \right] \frac{E}{1000}; \quad (3)$$

$I_0$  is the saturation current

$$I_0 = I_{rs} \cdot \left( \frac{T}{T_n} \right)^3 \cdot e^{\frac{q \cdot E_{g0}}{n \cdot K} \left( \frac{1}{T_n} - \frac{1}{T} \right)}; \quad (4)$$

$I_{rs}$  is the reverse saturation current

$$I_{rs} = \frac{I_{sc} k_i (T - 298)}{e^{\frac{q \cdot V_{oc} k_i (T - 298)}{n \cdot n_s \cdot K \cdot T}} - 1}; \quad (5)$$

$I_{sh}$  is the shunt resistor current

$$I_{sh} = \frac{V_p + I_p \cdot R_s}{R_{sh}}, \quad (6)$$

where  $I_{sc}$  is a short-circuit current, A;  $V_{oc}$  is the open circuit voltage, V;  $V_p$  is the working voltage of the PV module, V;  $k_i =$

$= 0.04$  is the temperature coefficient of short-circuit current reduction for a photocell at a temperature of  $25^\circ\text{C}$  and the energy flow density of  $1000 \text{ W/m}^2$ ,  $\%/^\circ\text{C}$ ;  $k_v = 0.3$  is the temperature coefficient of the open circuit voltage reduction for the photocell at the temperature of  $25^\circ\text{C}$  and the intensity (or power intensity) of the solar radiation of  $1000 \text{ W/m}^2$ ,  $\%/^\circ\text{C}$ ;  $T$  is the current temperature, K;  $T_n$  is the nominal temperature, K;  $E$  is the solar radiation intensity,  $\text{W/m}^2$ ;  $q = 1.6 \cdot 10^{-19}$  is the elementary electric charge, C;  $n = 0.546$  is the indicator of the diode idealization;  $K = 1.38 \cdot 10^{-23}$  is the Boltzmann constant, J/K;  $E_{g0} = 1.1$  is the semiconductor band gap, eV;  $n_s$  is the number of serially connected photovoltaic cells in the module;  $R_s = 0.309$  is series resistance,  $\Omega$ ;  $R_{sh} = 415.405$  is shunt resistance,  $\Omega$ .

The difference between the model considered in this work and the one proposed in [13] is that the temperature coefficient  $k_v$  is taken into account to construct volt-ampere characteristics.

Characteristics such as  $I_{sc}$ ,  $V_{oc}$ ,  $E$ ,  $T$ ,  $n_s$ ,  $k_i$ ,  $k_v$  are the most decisive for the photomodule. The unit settings window sets these characteristics for the photo module type Solarday SDM72 360 W used for shaping the photovoltaic arrays of the solar power plant.

Fig. 3 shows a comparison of the voltage-ampere characteristics of the solar photovoltaic module constructed using the Matlab model with the characteristics stated by the manufacturer for this type of PV module. Analysis of the obtained characteristics confirms the adequacy of the model developed.

The calculated volt-ampere characteristics of the photoelectric converter according to relations (2–6) are used in an adjustable current source, whose terminals are output to an external electrical circuit. The voltage sensor on the current source terminals measures the current value of the operating voltage of the PV module, which is used to calculate the operating current through the feedback circuit.

As is well known, the energy characteristics of a photovoltaic converter largely depend on the current surface tempera-

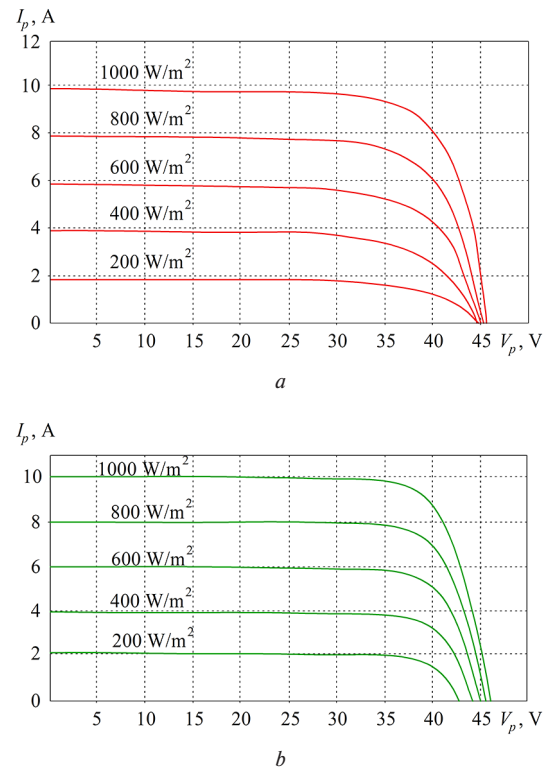


Fig. 3. Volt-ampere characteristics of the Solarday SDM72 360W PV module:

a – given in the manufacturer's catalog [19]; b – obtained using the Matlab-model for different specific power values



ture, with the increase of which the generation of electrical energy decreases. Therefore, to obtain the thermal characteristics of the selected Solarday SDM72 360 W PV module and assess the temperature impact on its operation during the creation of the Matlab-model, a laboratory experiment was conducted.

Fig. 4 shows photographs of the laboratory facility, with which temperature characteristics were obtained.

The test bench consists of a PV module type Solarday SDM72 360 W, two load rheostats and two powerful lighting fixtures with halogen lamps (rated power of one lamp is 2 kW), simulating a solar radiation source. The following tools were used for measurements: two digital multimeters MY75, used as a voltmeter and ammeter, respectively, digital luxmeter WT81, contactless infrared digital pyrometer ThermoSpot Pocket, digital oscilloscope SDS1022D.

The experiment was set up as follows. The lighting fixtures were placed so as to achieve the most uniform distribution of the light flux on the PV module surface. The level of illumination at the control points of the surface was monitored by a digital light meter WT81. The ThermoSpot Pocket digital non-contact pyrometer was mounted and fixed on a rack between two luminaires so that the temperature in the center of the PV module to be continuously monitored during the experiment. The  $R_H = 40 \Omega$  load resistance was set using rheostats. Before the experiment, the laboratory room was ventilated and then heated to exclude convective airflows, the current temperature at the central point of the photovoltaic module, the idle voltage and short-circuit current during nominal operation of both light sources were measured.

The photovoltaic module was then coupled to the load rheostats, which switched the unit to steady-state conditions, under which it operated throughout the experiment. To eliminate the observer influence on the measurement process, the readings of the measuring instruments were recorded by synchronized digital video cameras.

Fig. 5 shows a comparison of the measurement results with the results of a computer experiment conducted using the Matlab-model of the Solarday SDM72 360 W PV module, presented as the dependences of the power output on the temperature when changing the latter from 25 to 55 °C.

As can be seen from Fig. 5, the obtained experimental data are highly correlated with the results of computer simulation, which makes it possible to use the synthesized Matlab-model of the Solarday SDM72 360 W PV module to build a simulation model of SPP.

The payback period for the capital costs of building a solar power plant will depend on the annual amount of electricity generated. Therefore, many network inverters have a maximum power selection function (MPP) [13, 16]. To implement this mode, an MPP tracker was synthesized, the Matlab model of which is shown in Fig. 6. The tracker performs two basic



Fig. 4. Appearance of the laboratory facility used for experimental measurements

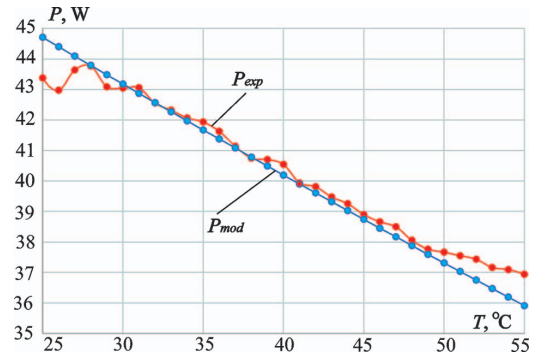


Fig. 5. Dependences of the power output of the Solarday SDM72 360 W PV module on the temperature according to the experimental results ( $P_{exp}$ ) and computer simulation ( $P_{mod}$ )

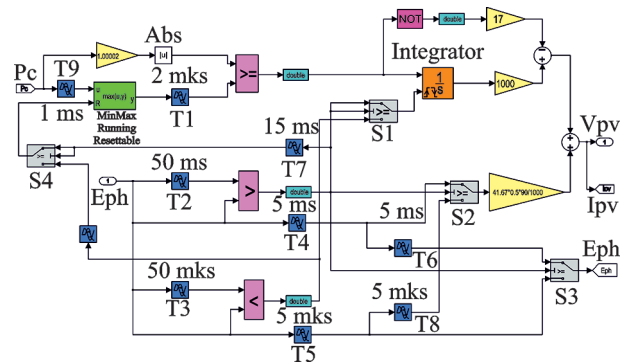


Fig. 6. Matlab-model of the MPP tracker

functions: tracking the point of maximum power with regard to the volt-ampere characteristic of the solar module and ensuring the dynamics of transition between the said characteristics during natural changes in solar radiation intensity during the solar module operating time.

The Matlab-model, which implements the algorithm of MPP tracker, consists of a node for maximum power point tracking and nodes for adjusting the system to change the solar radiation intensity. The maximum power point tracking node, in turn, consists of a MinMax Running Resettable, a logical operator greater than or equal to ( $> =$ ), which compares the modulus of the current value of the measured power output with the maximum power output value that comes from MinMax Running Resettable, the Integrator, and inverting logic operator (NOT), which is used in the feedback loop of the integrator to account for system's transients. Units T1, T9 are used to set the appropriate delays in the input and output circuits of the MinMax Running Resettable unit.

The maximum power point tracking node operates as follows. The logic operator ( $> =$ ) compares the current value modulus of the measured power at the output of the solar photovoltaic module (or photovoltaic array) with the maximum value of the measured power output stored in the memory cell (MinMax Running Resettable unit) supplied to the corresponding input of the logical operator with a delay  $T1 + T9$ . If the conditions of this inequality are met, a logic unit is set at the output of the logic operator unit and an integrator is started, which increases the value of the reference signal for the DC/DC step-down converter or for the transistor inverter that regulates the capacitor voltage. Thus, the controller operates with a nonlinear drooping section of the photoelectric converter volt-ampere characteristic, while the working point is raised by this section.

The movement of the operating point is accompanied by a decrease in the output voltage and an increase in the output

current of the PV module, while the value of the output power increases. The increase in output power will be maintained until its maximum value is reached, which will lead to a violation of the inequality in the logical operator unit ( $>=$ ), which will switch and change to logical 0 state. Changing the state will stop the integrator (Integrator unit) and switch the inverting NOT unit from the logical 0 state to the logical unit state. The final switching will slightly reduce the calculated reference signal, which adjusts for the inertia of the step-down converter after stopping the integrator, stabilizes the maximum value of power at the output of the photoelectric converter and prevents the inverter from overturning.

The nodes of the system adjustment to change the specific power of solar radiation respond to changes in natural illumination by the signal Eph. If the current signal has decreased or increased relative to the previous value, then for a short time (determined by the delay T2 or T3) one of the logical operators starts ( $> -$  in case of signal decrease) or ( $< -$  in case of signal increase). The logical unit at the input of the operator blocks ( $>$ ) and ( $<$ ) switches the keys S1–S4, which results in resetting the integrator and cleaning the memory cell that stores the maximum value of the measured power (MinMax Running Resettable block). The control system is then returned to the working condition and a new maximum power value is searched using the above algorithm.

In the first step, the algorithm and the proposed MPP tracker model were tested using the Matlab-model of the Solarday SDM72 360 W PV module. The Table shows the results of the maximum power point tracking at different solar radiation intensity values.

The development of a full-scale model of the solar photovoltaic station with a converter system based on a multi-level cascade voltage inverter with MPP function should begin with the synthesis of an intermediate model of one converter cell. Let us replace the inverter cell with a three-phase transistor inverter, which supplies 1/42 of energy produced by the powerful solar power plant to the industrial network.

The model is composed of a photoelectric array of solar modules, which are arranged in 18 parallel rows (strings) of 32 PV modules type Solarday SDM72 360 W in each. The installed power of the array is 200 kW. Capacitor C is connected in the DC circuit, whose voltage is maintained within the following limits

$$U_c = \frac{(1.25 \dots 1.5) \sqrt{2} U_{line}}{14}.$$

A power inverter implemented according to a three-phase bridge circuit on IGBT transistor base is connected to the DC link. The inverter alternating current link and the power supply network are connected through an inductance reactor.

The key element of the model is the inverter control system, which implements the MPPT function (Fig. 7). The model is derived from vector principle of control shaping, which applies the coordinate conversion of modern power theory, namely  $abc \rightarrow dq0$  and inverse transformations of  $dq0 \rightarrow abc$  coordinates [21].

The control system operates as follows. At the input of the coordinate conversion units (Discrete 3-phase PLL,  $abc\_to\_dq0$  Transf), the scaling amplifier receives information from sensors on the instantaneous voltage values in the three-phase supply line  $u_a, u_b, u_c$ , where conversion of the latter occurs

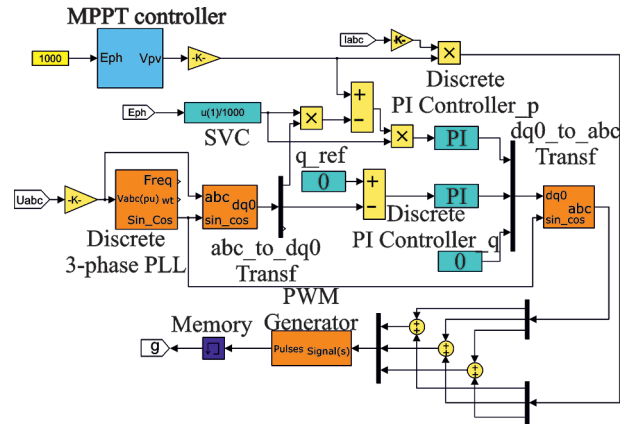


Fig. 7. Photovoltaic station inverter control system model

$$\begin{bmatrix} u_d \\ u_q \\ u_0 \end{bmatrix} = \begin{bmatrix} \frac{\sqrt{2} \cos \theta_1}{\sqrt{3}} & \frac{\sin \theta_1}{\sqrt{2}} - \frac{\cos \theta_1}{\sqrt{6}} & -\frac{\sin \theta_1}{\sqrt{2}} + \frac{\cos \theta_1}{\sqrt{6}} \\ -\frac{\sqrt{2}}{3} \sin \theta_1 & \frac{\sin \theta_1}{\sqrt{6}} + \frac{\cos \theta_1}{\sqrt{2}} & \frac{\sin \theta_1}{\sqrt{6}} - \frac{\cos \theta_1}{\sqrt{2}} \\ \frac{1}{\sqrt{3}} & \frac{1}{\sqrt{3}} & \frac{1}{\sqrt{3}} \end{bmatrix} \begin{bmatrix} u_a \\ u_b \\ u_c \end{bmatrix}.$$

The angle  $\theta_1$  is determined from the ratio

$$\theta_1 = \arctg\left(\frac{u_\beta}{u_\alpha}\right) = \arctg\left(\sqrt{3} \frac{u_b - u_c}{2u_a - u_b - u_c}\right).$$

Simultaneously, the MPP tracker (MPP tracker unit) calculates the  $V_{pv}$  voltage problems according to the algorithm considered, which corresponds to the maximum power point tracking, which, through the scaling amplifier, enters the input of the comparison unit with the projection of the voltage vector on the  $p$  axis  $-u_p$ . The difference signal is received at the input of the proportional-integral controller (Discrete PI Controller\_p unit), whose output is connected to the input of the unit of inverse coordinate conversion ( $dq0\_to\_abc$  Transf). If the power plant is to be involved into the reactive power regulation in the grid, the input of the coordinate transformation unit ( $dq0\_to\_abc$  Transf) must also receive a signal from the proportional-integral controller (Discrete PI Controller\_q unit) for the voltage vector component on the  $q$  axis. Otherwise, this power port can be disconnected.

The operation of the inverse coordinate conversion unit ( $dq0\_to\_abc$  Transf) is described by the following relations

$$\begin{bmatrix} i_{aref} \\ i_{bref} \\ i_{cref} \end{bmatrix} = \begin{bmatrix} \frac{\sqrt{2} \cos \theta_1}{\sqrt{3}} & -\frac{\sqrt{2}}{3} \sin \theta_1 \\ \frac{\sin \theta_1}{\sqrt{2}} - \frac{\cos \theta_1}{\sqrt{6}} & \frac{\sin \theta_1}{\sqrt{6}} + \frac{\cos \theta_1}{\sqrt{2}} \\ \frac{\sin \theta_1}{\sqrt{2}} + \frac{\cos \theta_1}{\sqrt{6}} & \frac{\sin \theta_1}{\sqrt{6}} - \frac{\cos \theta_1}{\sqrt{2}} \end{bmatrix} \begin{bmatrix} i_{d^*} \\ i_{q^*} \end{bmatrix},$$

where

$$i_{d^*} = \left( V_{pv} K_0 - \frac{E_{ph} u_d}{1000} \right) \frac{E_{ph} K_{pd}}{1000} + \frac{K_{id} E_{ph}}{1000 T_i} \int \left( V_{pv} - \frac{E_{ph} u_d}{1000} \right) dt;$$

$$i_{q^*} = (u_{qref} - u_q) K_{pq} + \frac{K_{iq}}{T_i} \int (u_{qref} - u_q) dt,$$

where  $K_{pd}, K_{qd}, K_{id}, K_{iq}$  are proportional and integral amplification coefficients of the two PI-controllers respectively;  $T_i$  is the integration period;  $K_0 = 1/(0.5 V_{oc} \cdot N_s)$  is the coefficient.

Table

Test of maximum power point tracking algorithm using the Matlab-model of the Solarday SDM72 360 W PV module

$E_{ph}, W/m^2$	200	400	600	800	1000
$P_{max}, W$	68.56	142.8	217	289.4	360.7

The phase current reference of the inverter is obtained after a phase comparison of the reference current with the measured currents of the grid in the feedback circuit

$$\begin{bmatrix} i_{a^*} \\ i_{b^*} \\ i_{c^*} \end{bmatrix} = \begin{bmatrix} i_{aref} + i_a V_{pv} K_0 \\ i_{bref} + i_b V_{pv} K_0 \\ i_{cref} + i_c V_{pv} K_0 \end{bmatrix}.$$

Synthesis of the Matlab-model of solar photovoltaic station with a transformerless multi-level voltage inverter (Fig. 2) is the final simulation stage, summing up the results of the three previous stages.

The structure of the multi-level converter control system follows the previously considered structure of the vector control system of the ordinary three-phase bridge voltage inverter with the MPPT function (Fig. 7), but its operation has been extended by the system for distributing impulses to inverter cells of the converter, the operation of which has been analyzed in detail in [18].

The pulse distribution system presents a symmetrical structure, formed by 42 single-item PWM cells (14 cells per phase) operating at a constant modulation rate, their operation being shifted by an angle in time

$$\varphi_0 = \frac{n_L \cdot \pi}{3},$$

where  $n_L = 1, 2, 3, \dots, k-1$ ,  $k$  is the number of cells in the inverter phase.

The PWM generator generates vertical levels of high-frequency saw-toothed voltage “0 + 1” and “0 – 1” and compares them with the reference input signal. Pulse reallocation to transistor cells is performed according to the switching Table [18].

Fig. 8 shows the oscillograms that demonstrate the Matlab-model of a photovoltaic station with a rated power of 8.4 MW based on a 29-level transformer-free cascade voltage converter. The oscillograms are obtained by changing the solar radiation intensity from 1000 to 500 W/m<sup>2</sup>.

The analysis of Fig. 8 gives an idea of the correct operation of the solar power plant model, both in the steady state and in the transition mode. The control system performs the jumping variation of the solar radiation intensity in a pronounced way; the algorithm of maximum possible power point tracking finds the required output power value, which makes it possible to increase the operation efficiency of the power plant equipment and to reduce the period of repayment of capital investment on its construction. Studies confirm the significant advantage of multi-level schemes in obtaining qualitative indicators of electrical energy generated for the electric network, i.e. network currents are symmetric, sinusoidal ( $THD_I < 5\%$ ) and are in antiphase with the corresponding phase voltages.

#### Conclusions.

1. The key structural advantage of the converting system operating circuit of the distributed SPP based on the multilevel

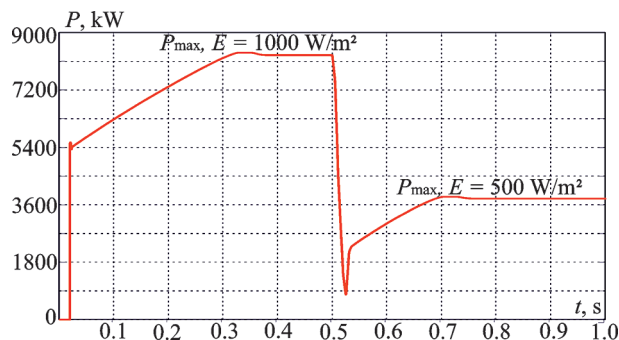


Fig. 8. Timing of the output power of the SPP when the intensity of solar radiation change from 1000 to 500 W/m<sup>2</sup>

cascade voltage inverter in comparison with known technical solutions is the absence of the network transformer 10(6)/0.4 kV. Of course, this advantage is partly offset by the need to use a high-voltage grid reactor, but given that traditional inverter circuits likewise require the use of grid-side induction reactors (in most cases the transformer-leakage inductance is not sufficient for the correct converter operation), the proposed solution is very promising from the point of view of recouping investments in the construction of industrial SPP.

2. In the Matlab/Simulink/SimPowerSystems environment, a Solarday SDM72 360 W PV module model with real electrical and thermal characteristics is synthesized. The dependence of the PV module output capacity on the surface temperature of the module has been tested using a laboratory unit. It is established that both the calculated and experimental characteristics obtained correspond to the characteristics stated by the manufacturer.

3. An algorithm is proposed and an MPP-tracker with volt-ampere characteristics of the PV module corresponding to the maximum power extraction is synthesized based on the said algorithm. The algorithm was tested using the above model and proved to be effective for all solar radiation intensity values.

4. A model of the solar power plant with a converter system based on a three-phase transistor voltage inverter simulates the operation of a single cell of the multi-level converter. The model allowed testing the algorithm for maximum power point tracking (MMPT) of the photoelectric array to be generated by 576 Solarday SDM72 360 W PV modules.

5. Synthesized is the Matlab-model of solar photovoltaic station with transformer-free 13-level cascade voltage inverter with rated power of 8.4 MW in the maximum power extraction mode. The model confirmed the efficiency and effectiveness of the converter system and the power plant as a whole. Model results show the prospect of future commercial application of transformerless multi-level converter systems to be used in the structure of powerful solar photovoltaic stations.

The findings of the publication were obtained in the framework of the state budget research work 53-73/19 “Development of Scientific Fundamentals for Introduction of Intelligent Energy Efficient Power Supply Systems SmartGrid”, No. DR 0119U001072.

#### References.

- Tugay, D., Kotelevets, S., Korneliuk, S., & Zhemerov, G. (2018). Energy efficiency of microgrid implementation with solar photovoltaic power plants. *2018 IEEE 3<sup>rd</sup> International Conference on Intelligent Energy and Power Systems*, 275-279. <https://doi.org/10.1109/IEPS.2018.8559579>.
- Almasi, H., Panterlis, J., & Alian, M. (2019). Comparison Between two 10MW Solar Plant with Central and Distributed Inverters. *2019 27<sup>th</sup> Iranian Conference on Electrical Engineering (ICEE)*, Yazd, Iran, 831-835. <https://doi.org/10.1109/IranianCEE.2019.8786627>.
- Rabiul, I. M., Mahfuz-Ur-Rahman, A. M., Muttaqi, & Sutan-to, K. M. (2019). State-of-the-Art of the Medium-Voltage Power Converter Technologies for Grid Integration of Solar Photovoltaic Power Plants. *IEEE Transactions on Energy Conversion*, 34(1), 372-384. <https://doi.org/10.1109/TEC.2018.2878885>.
- Foureaux, N. C., Adolpho, L., Silva, S. M., Brito, J. A., & Cardoso Filho, B. (2014). Application of solid state transformers in utility scale solar power plants. *2014 IEEE 40<sup>th</sup> Photovoltaic Specialist Conference (PVSC)*, 3695-3700. <https://doi.org/10.1109/PVSC.2014.6924909>.
- Ahmad, S., Johari, S. H., Ahmad, A., & Halim, M. F. (2015). Grid connected multilevel inverters for PV application. *2015 IEEE Conference on Energy Conversion (CENCON)*, 181-186. <https://doi.org/10.1109/CENCON.2015.7409536>.
- Abdalla, I., Corda, J., & Zhang, L. (2012). Multilevel DC-Link Inverter and Control Algorithm to Overcome the PV Partial Shading. *IEEE Transactions on Power Electronics*, 28(1), 14-18. <https://doi.org/10.1109/TPEL.2012.2209460>.
- Agarwal, R., & Jain, S. (2016). A new multilevel inverter for grid connection of PV modules. *2016 IEEE 7<sup>th</sup> Power India International Conference*, 1-6. <https://doi.org/10.1109/POWERI.2016.8077194>.



8. Plakhtii, O., Nerubatskyi, V., Khomenko, I., Tsybulnyk, V., & Syniavskyi, A. (2020). Comprehensive study of cascade multilevel inverters with three level cells. *2020 IEEE 7<sup>th</sup> International Conference on Energy Smart Systems*, 277-282. <https://doi.org/10.1109/ESS50319.2020.9160258>.
9. Plakhtii, O., Nerubatskyi, V., Sushko, D., Hordienko, D., & Khoruzhevskiy, H. (2020). Improving the harmonic composition of output voltage in multilevel inverters under an optimum mode of amplitude modulation. *Eastern-European Journal of Enterprise Technologies*, 8(104), 17-24. <https://doi.org/10.15587/1729-4061.2020.200021>.
10. Bangaraju, J., Rajagopal, V., Bhoopal, N., & Priyanka, M. (2014). Power quality improvement using solar PV H-bridge based hybrid multilevel inverter. *2014 IEEE 6<sup>th</sup> India International Conference on Power Electronics*, 1-5. <https://doi.org/10.1109/IICPE.2014.7115841>.
11. Hosseinzadeh, M. A., Sarbanzadeh, M., Munoz, J., Rivera, M., Munoz, C., & Villalon, A. (2019). New Reduced Switched Multilevel Inverter for Three-Phase Grid-Connected PV System, Performance Evaluation. *2019 IEEE International Conference on Industrial Technology*, 1488-1493. <https://doi.org/10.1109/ICIT.2019.8755112>.
12. Kumar, S., & Pal, Y. (2019). A Three-Phase Asymmetric Multilevel Inverter for Standalone PV Systems. *2019 6<sup>th</sup> International Conference on Signal Processing and Integrated Networks*, 357-361. <https://doi.org/10.1109/SPIN.2019.8711605>.
13. Katkamwar, S. S., & Doifode, V. R. (2016). Cascaded H-bridge multilevel PV inverter with MPPT for grid connected application. *2016 International Conference on Energy Efficient Technologies for Sustainability*, 641-646. <https://doi.org/10.1109/ICEETS.2016.7583832>.
14. Uthirasamy, R., Ragupathy, U. S., Megha, C., & Mithra, R. (2014). Design and analysis of three phase modified cascaded multilevel inverter for PV applications. *2014 International Conference on Green Computing Communication and Electrical Engineering*, 1-6. <https://doi.org/10.1109/ICGCCEE.2014.6922441>.
15. Plakhtii, O., Nerubatskyi, V., Karpenko, N., Ananieva, O., Khoruzhevskiy, H., & Kavun, V. (2019). Studying a voltage stabilization algorithm in the cells of a modular six-level inverter. *Eastern-European Journal of Enterprise Technologies*, 8(102), 19-27. <https://doi.org/10.15587/1729-4061.2019.185404>.
16. Aute, S. R., & Naveed, S. A. (2019). Simulation and Analysis of Multilevel Inverter Based Solar PV System. *2019 3<sup>rd</sup> International Conference on Computing Methodologies and Communication*, 557-559. <https://doi.org/10.1109/ICCMC.2019.8819742>.
17. Kiran, R., Jayaraman, M., & Sreedevi, V. T. (2014). Power quality analysis of a PV fed seven level cascaded H-bridge multilevel inverter. *2014 IEEE International Conference on Advanced Communications, Control and Computing Technologies*, 281-285. <https://doi.org/10.1109/ICACCCT.2014.7019446>.
18. Zhemerov, G. G., Tugay, D. V., & Titarenko, I. G. (2013). Simulation of AC drives system comprising multilevel inverter. *Electrotechnics and electromechanics*, 2, 40-47.
19. *SolarDay. Modules and technology* (n.d.). Retrieved from [https://www.solarday.it/new/wp-content/uploads/2018/07/SOLARDAY\\_EN\\_SDM72-340-360.pdf](https://www.solarday.it/new/wp-content/uploads/2018/07/SOLARDAY_EN_SDM72-340-360.pdf).
20. Beshta, O., Kuvaiiev, V., Mladetskiy, I., & Kuvaiiev, M. (2020). Ulpa particle separation model in a spiral classifier. *Naukovyi Visnyk Natsionalnoho Hirnychoho Universytetu*, (1), 31-35. <https://doi.org/10.33271/nvngu/2020-1/031>.
21. Tugay, D., Kolontaievskiy, Y., Korneliuk, S., & Akymov, V. (2020). Comparison of the compensation quality for active power filter control techniques. *2020 IEEE KhPI Week on Advanced Technology*, 236-241. <https://doi.org/10.1109/KhPIWeek51551.2020.9250092>.

## Моделювання промислової сонячної фотоелектричної станції з безтрансформаторною перетворювальною системою

Д. В. Тугай, С. І. Корнелюк, О. О. Шкурпела,  
В. С. Акимов

Харківський національний університет міського господарства імені О. М. Бекетова, м. Харків, Україна, e-mail: [tugaydmytro@gmail.com](mailto:tugaydmytro@gmail.com)

**Мета.** Створення детальної моделі сонячної фотоелектричної станції з перетворювальною системою на основі каскадного багаторівневого інвертора з функцією МРРТ для дослідження її режимів роботи в розподілених системах електропостачання.

**Методика.** Для проведення дослідження в роботі використовувалися методи синтезу систем, математичного й комп'ютерного моделювання під час створення моделей фотоелектричної станції та її елементів; фізичного експерименту під час отримання теплових характеристик фотоелектричного модулю Solarday SDM72 360W; сучасні теорії потужності для синтезу векторної системи керування багаторівневим інвертором.

**Результати.** Синтезована Matlab-модель сонячної фотоелектричної станції з безтрансформаторним 29-рівневим каскадним інвертором напруги. Модель підтвердила працездатність і ефективність роботи перетворювальної системи та електростанції в цілому. Запропоновано алгоритм і синтезовано на його основі контролер пошуку робочої точки на вольт-амперних характеристиках фотомодуля, що відповідає відбору максимальної потужності. Перевірка алгоритму за допомогою моделі підтвердила його працездатність за будь-яких значень інтенсивності потужності сонячного випромінювання.

**Наукова новизна.** Отримана повна математична модель фотоелектричного модуля, що враховує його енергетичні й теплові характеристики та може бути використана для імітації роботи будь-якої комп'ютерної моделі фотоелектричного перетворювача в середовищі Matlab/Simulink/SimPowerSystems.

**Практична значимість.** Результати моделювання свідчать про перспективність промислової реалізації безтрансформаторних багаторівневих перетворювальних систем для їх використання у структурі потужних сонячних фотоелектричних станцій.

**Ключові слова:** фотоелектричний модуль, сонячна фотоелектрична станція, багаторівневий інвертор, перетворювальна система, МРР контролер

*Recommended for publication by V. G. Yagup, Doctor of Technical Sciences. The manuscript was submitted 22.02.21.*